

# **High Power Reciprocal Ferrite Switches Using Latching Faraday Rotators**

**Charles R. Boyd, Jr.  
Microwave Applications Group  
Santa Maria, California, USA**

**IEEE S-MTT International Microwave Symposium  
Workshop: Issues in Ferrites and Dielectrics  
for High Power Applications  
Philadelphia, PA, June, 2003**

# High Power Reciprocal Ferrite Switches Using Latching Faraday Rotators

Charles R. Boyd, Jr.  
Microwave Applications Group  
Santa Maria, California, USA

## 1. Introduction

Faraday Rotation is the simplest and most intuitive way in which microwaves interact with a magnetized ferrite medium. Consequently it is also one of the oldest phenomena used for construction of practical microwave ferrite components. The approach was already well known by 1956 when Ohm [1] presented a paper discussing an optimized version of a four-port circulator based on Faraday Rotation. He used the following sketch to show the physical layout of the device:

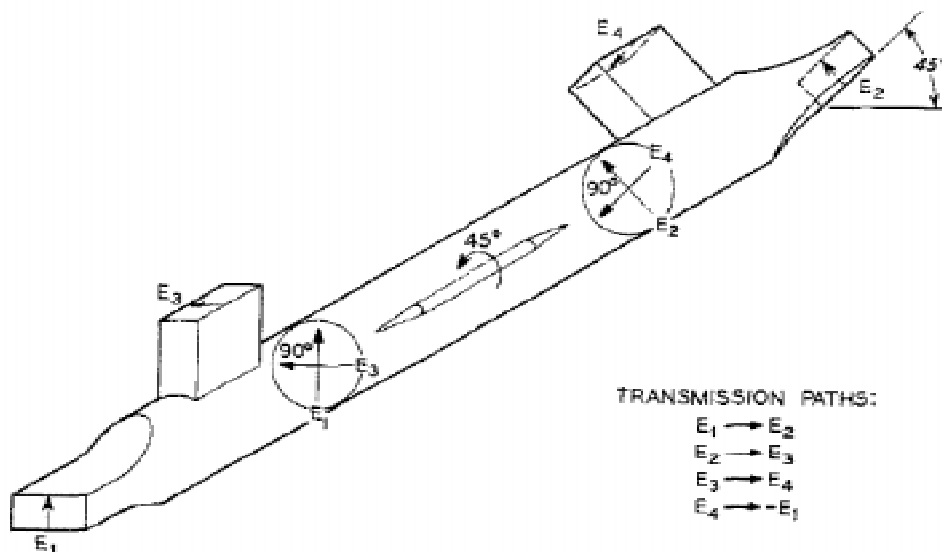
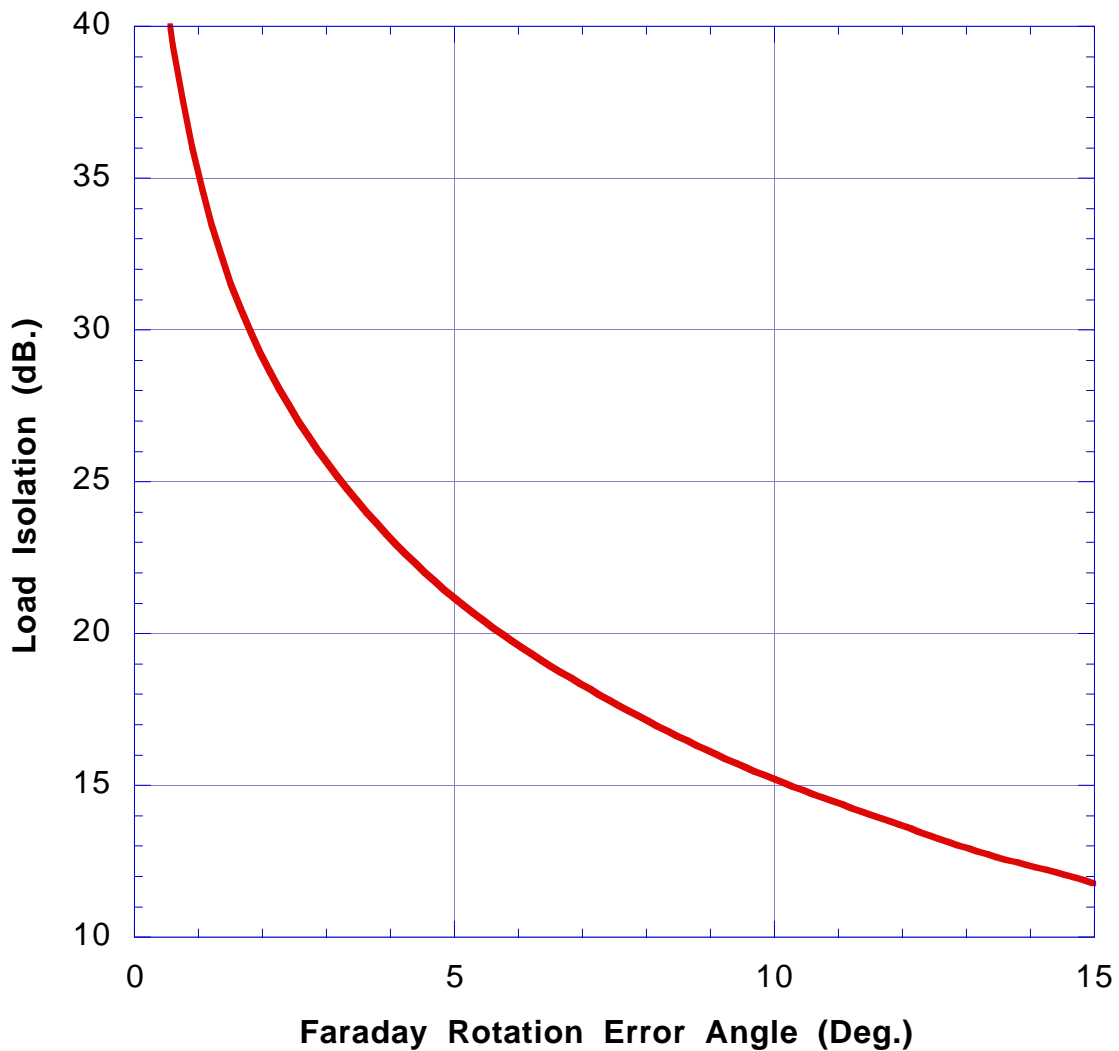


Fig. 1—An ideal circulator.

This device used a slender rod of ferrite “floating” in a cylinder of polystyrene foam, which in turn was fitted into a circular waveguide with a sleeve of solid polystyrene lining the interior walls of the guide. The operating frequency range was 10.7 to 11.7 GHz., and the length of the ferrite rod was 3.85 inches (97.79 mm.), plus linear tapers of one inch (25.4 mm.) at each end. A bias field of 200 Oersteds was required to magnetize the ferrite to the level required for optimum performance. An insertion loss of 0.19 dB. and isolation greater than 30 dB. were achieved.

Clearly, the sequence of coupled ports can be inverted by reversing the direction of the applied longitudinal magnetic bias field, and so this type of circulator can be adapted to form a nonreciprocal switch. The amount of rotation required is only  $\pm 45^\circ$ , so that with proper choice of material and careful design, a low insertion loss is possible. In addition to being nonreciprocal rather than reciprocal, this basic configuration could be improved by (a) better heat transfer from the ferrite rod to the external structure, and (b) a closed magnetic path for the bias field to permit fast, latching operation. An intrinsic problem with this kind of device is the fact that deviations of the Faraday Rotation angle from the optimum  $45^\circ$  value cause power to be coupled to the isolated port. The magnitude of the coupled power increases as the sine of the error angle, and Figure 2 shows the degraded isolation in decibels as a function of the error angle magnitude. It is



**Fig. 2 - Circulator OFF Port Isolation vs. Faraday Rotation Error Angle**

evident that in order to maintain an isolation of at least 30 dB., the error angle must not be allowed to exceed about 1.8 degrees, which corresponds to a deviation tolerance of about 4 percent of the optimum rotation amount. This is a really difficult level of precision to achieve and maintain over a significant frequency band and over a wide operating temperature range.

It is fairly obvious that a reciprocal switch can be achieved by placing two identical switchable 90-degree Faraday Rotators in a waveguide bridge, as depicted in the block diagram of Figure 3. Since the rectangular waveguides coupling to the inputs and outputs of the 90-degree rotators will be cross-polarized, a compact bridge is realized by using an E-plane folded hybrid tee at one end of the bridge and an H-plane folded hybrid tee at the other end. What is perhaps less obvious is that any small deviations in the amount of Faraday Rotation from the optimum 90-degree value will appear as a small field component cross-polarized to the desired output. This cross-polarized field can be absorbed in a film load, and consequently an accurate zero-degree or 180-degree switchable phase relationship of equal-amplitude waves will be presented to the combining hybrid tee over a moderate range of temperatures and frequencies. In effect, small errors of Faraday Rotation are converted to small increases of insertion loss and do not degrade the isolation of the switch; isolation levels in excess of 30 dB. are readily achievable and maintainable over moderate temperature and frequency variation.

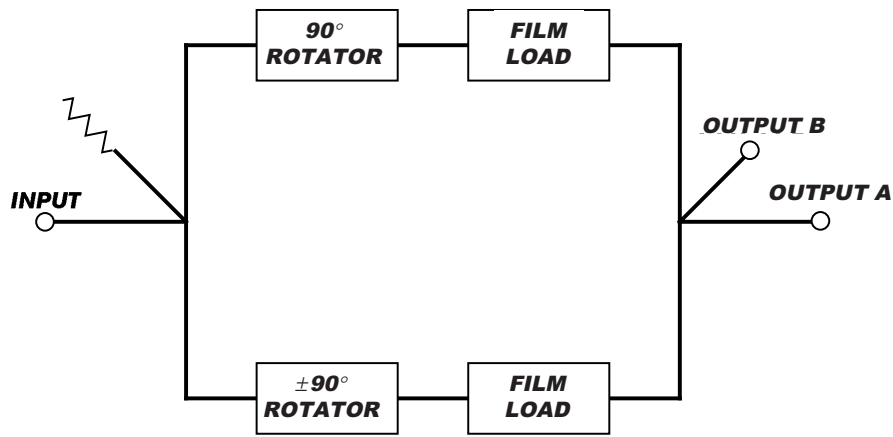


**Fig. 3 - Simple Bridge-Type Faraday Rotation Reciprocal Switch**

The amplitude of the signal coupled to the desired output port will vary as the cosine of the deviation of the Faraday Rotation angle from the optimum  $90^\circ$  value. That is, an increase of insertion loss above the level produced by transducer and ferrite material losses will be caused by coupling of power to the film loads. Figure 4 below shows a plot of the added insertion loss in decibels as a consequence of error of the Faraday Rotation amount.

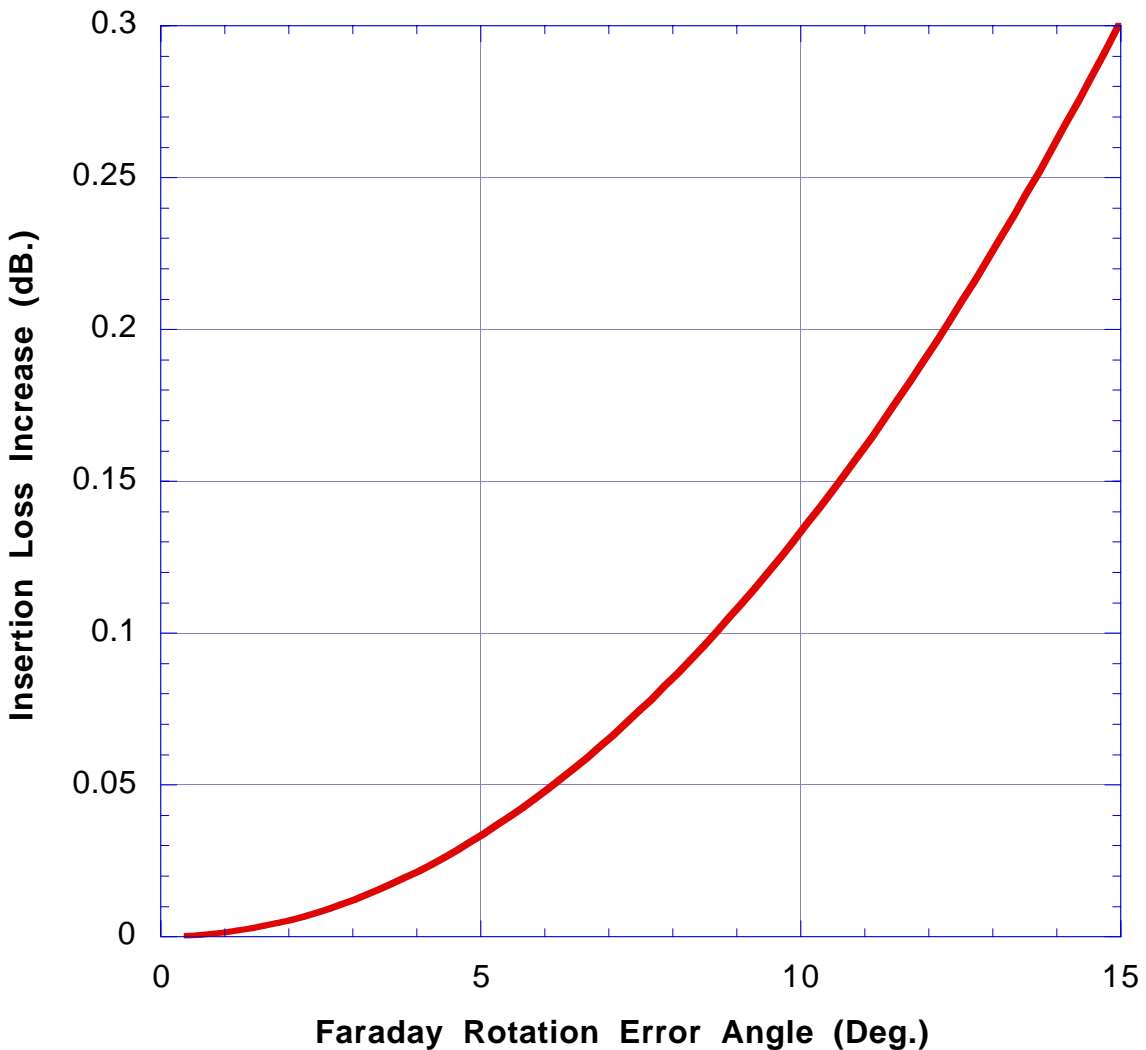


**Fig. 4 - Insertion Loss Increase vs. Faraday Rotation Error Angle**

Suppose that an increase of 0.1 dB. of insertion loss is acceptable as a result of deviation of the Faraday Rotation angle from the optimum  $90^\circ$  value. Then the error angle magnitude can be as large as 8.68 degrees, which corresponds to 9.6 percent of the optimum  $90^\circ$  value. So it appears that shifting the critical parameter from isolation to insertion loss has caused the tolerance for the error angle to be relaxed, in spite of the fact that the optimum rotation angle has doubled in value, a necessary criterion for obtaining reciprocal behavior of the switch.

The block diagram of Figure 3 is based on the concept of using deposited-film resistors sputtered onto the dielectric transformers matching the ferrite rods to the input and output waveguides. For high power applications, loads of this type may be inadequate to handle the expected cross-polarized error power resulting from deviations of the Faraday Rotation angle from optimum. Figure 5 below shows a plot of the percentage of output power that will be delivered to the loads, as a function of the error angle. This is really the same plot as Figure 2, except that the y-axis is expressed as a normalized power level rather than an isolation level.

Whenever the potential power delivered to the loads is greater than that which can be handled comfortably by a film-type load, an alternative configuration is used in which the outputs of the Faraday Rotators are coupled into square waveguides. A pair of orthogonal-mode transducers is then used to extract the cross-

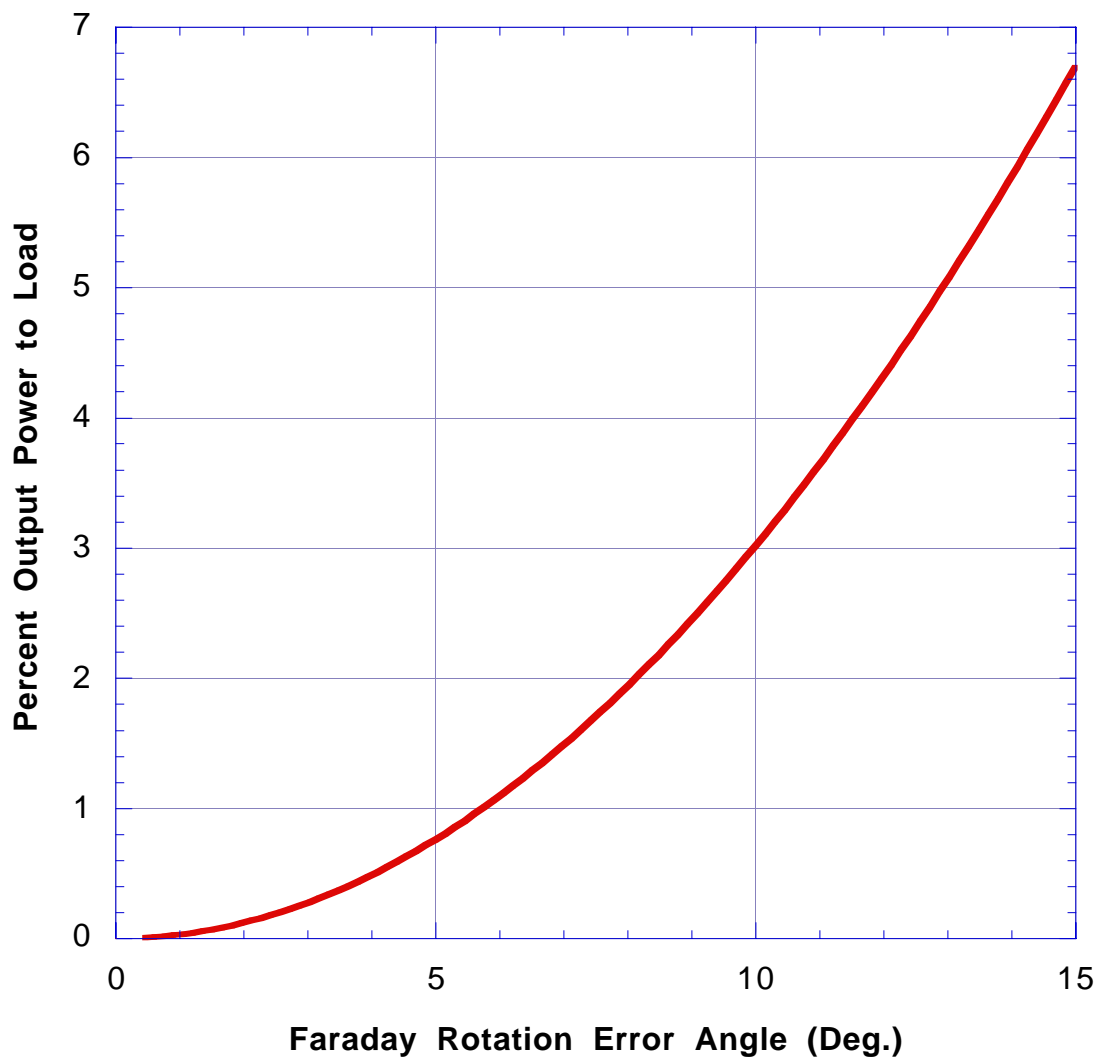


**Fig. 5 - Load Power vs. Faraday Rotation Error Angle**

polarized error power and apply same to loads with the appropriate power handling capability. Figure 6 below shows a block diagram of a more robust version of the basic bridge-type reciprocal switch using Faraday Rotators.

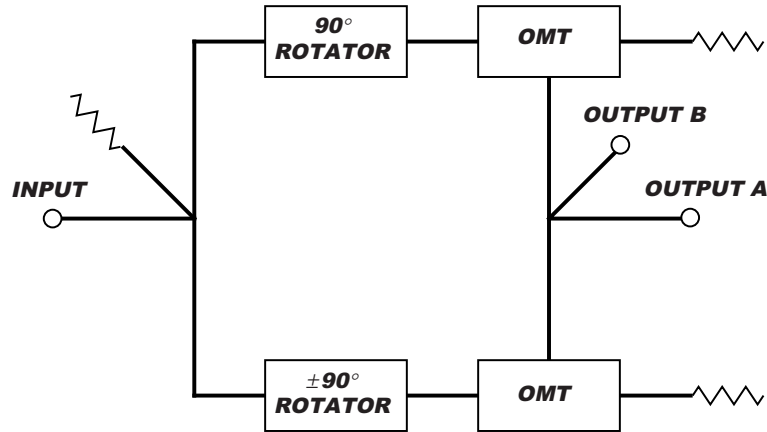


**Fig. 6 - Robust Bridge-Type Faraday Rotation Reciprocal Switch**

## 2. Faraday Rotator Design Considerations

The design of Faraday Rotators for switch applications is closely related to the design of dual-mode reciprocal ferrite phase shifters [2, 3]. Both devices operate with a square or round waveguide cross-section that is loaded with an axially symmetric ferrite rod. The dual-mode phase shifter operates with circular polarization, while the Faraday Rotator operates with linearly polarized waves. Since right-hand and left-hand circular polarization are the normal modes of the structure in the presence of a longitudinal magnetic bias field on the ferrite, waves will propagate along the dual-mode phase shifter structure without changing character. Waves propagating through a given structure length  $l$  will have an insertion phase angle change  $\beta l$ , where  $\beta$  is the propagation factor associated with the particular sense of circular polarization applied. The values of  $\beta$  for right-hand and left-hand circular polarization are commonly designated as  $\beta_+$  and  $\beta_-$ , respectively. Both  $\beta$  values are dependent on the ferrite material properties, structure dimensions, operating frequency, and the direction and magnitude of the longitudinal magnetic bias field. The numerical values of  $\beta_+$  and  $\beta_-$  are interchanged when the direction of the applied magnetic bias field are both reversed. The available phase shift  $\Delta\phi_{MAX}$  for a latching dual-mode phase shifter is given by

$$\Delta\phi_{MAX} = (\beta_{+MAX} - \beta_{-MAX}) l \tag{1}$$

where  $\beta_{+MAX}$  and  $\beta_{-MAX}$  are the limit values at the major hysteresis loop remanent magnetization points.

The linear polarization applied to the input of a Faraday Rotator can be expressed as a superposition of equal-amplitude right-hand and left-hand circularly polarized waves. These two normal-mode waves will propagate along the structure without changing character, but at generally different propagation constants. The Faraday Rotation angle  $\theta$  will be half the difference be-

tween the insertion phases of the two modes, i. e.

$$\theta = \frac{(\beta_+ - \beta_-) l}{2} \quad (2)$$

while the insertion phase  $\phi$  of the rotated wave will be the average of the insertion phases of the two normal modes:

$$\phi = \frac{(\beta_+ + \beta_-) l}{2} \quad (3)$$

The numerical values of  $\beta_+$  and  $\beta_-$ , and hence the direction of the rotation angle, are interchanged by a reversal of the direction of the applied magnetic bias field. Finally, the available rotation angle  $\theta_{MAX}$  for a latching Faraday Rotator will be

$$\theta_{MAX} = \frac{(\beta_{+MAX} - \beta_{-MAX}) l}{2} \quad (4)$$

where, as before,  $\beta_{+MAX}$  and  $\beta_{-MAX}$  are the limit values at major hysteresis loop remanence.

A typical low-power latching Faraday Rotator structure consists of a round waveguide filled with ferrite or ceramic of similar dielectric constant. The arrangement of ferrite and dielectric elements is shown in Figure 7. The center portion of the assembly is the switched ferrite, which is longitudinally magnetized to the desired level for a given amount of rotation. At the ends of the structure are dielectric sections containing thin resistive-film elements whose purpose is to absorb one sense of linearly polarized microwave energy, while allowing the orthogonal sense to pass with minimal insertion loss. This whole assembly is carefully metallized to form a waveguide. Impedance matching elements are used at the ends to couple to standard rectangular waveguides; for the usual case of 90 degree rotation, the input and output waveguides are cross-polarized. Finally, a ferrite yoke is fitted over the metallized surface in register with the central ferrite section to complete a closed magnetic path and thus permit latching operation of the phase shifter. From elementary magnetostatics, it is easily shown that a long and slender rod can be operated at remanent field values almost at the level of a solid toroid.

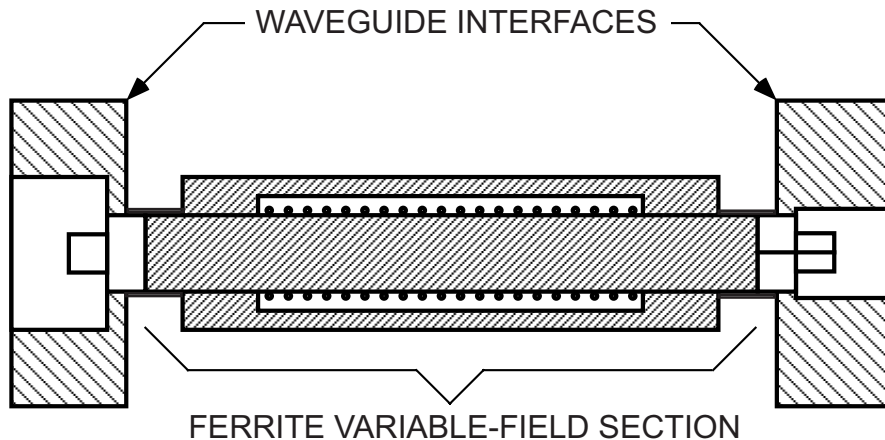


**Fig. 7 - Typical 90 Degree Faraday Rotator Configuration**

The basic design relationships for the latching dual-mode ferrite phase shifter have been previously presented in the literature [4]. Once the design equations have been incorporated into a computer program with the necessary modifications to deal with the Faraday Rotator case, it is quick and easy to try out many design variations and to examine the predicted performance for each case. Here is a printout of a typical trial design for a 90 degree rotator:

Round-Rod Faraday Rotator Parameters

Rod Diameter (In.)	0.3200
Number of Yoke Elements	2.0000
Yoke Gap Space (In.)	0.0200
Metal Wall Rel. Resistance	5.0000
Yoke-Rod Air Gap (In.)	0.0010
Start Frequency (GHz)	8.5000
Stop Frequency (GHz)	9.0000
Frequency Step (GHz)	0.0500

Rod and Yoke Material Properties

Rod Saturation Moment (G.)	800
Rod Rem. Flux Density (G.)	493
Rod Dielectric Constant	15.0000
Rod Coercive Force (Oe.)	1.0000
Rod H-Anisotropy (G.)	200
Rod Dielectric Loss Tangent	0.0002
Rod Magnetic Loss Tangent	0.0040
Rod Spinwave Linewidth (Oe.)	5.0000
Yoke Rem. Flux Density (G.)	1500
Yoke Coercive Force (Oe.)	1.0000

90 DEGREE FARADAY ROTATOR DESIGN DATA

CENTER FREQUENCY 8.750 GHZ

YOKE WINDOW LENGTH 1.117 INCHES  
YOKE PAD LENGTH 0.082  
TOTAL ROD LENGTH 1.280

YOKE WIDTH 0.320  
YOKE THICKNESS 0.041

PREDICTED BASE LOSS 0.12 DB. AT CENTER FREQUENCY

PERFORMANCE TABULATION

FREQUENCY (GIGAHERTZ)	ROTATION ANGLE (DEG.)	CROSS-POLARIZED MAGNITUDE (DB.)	INSERTION LOSS DB			
			COND	DIEL	MAG	TOTAL
8.500	88.26	-30.34	0.04	0.03	0.06	0.13
8.550	88.62	-32.38	0.04	0.03	0.06	0.13
8.600	88.98	-34.98	0.04	0.03	0.06	0.13
8.650	89.33	-38.59	0.04	0.03	0.06	0.12
8.700	89.67	-44.71	0.04	0.03	0.05	0.12
8.750	90.00	-293.03	0.04	0.03	0.05	0.12
8.800	90.33	-44.90	0.04	0.03	0.05	0.12
8.850	90.64	-38.97	0.04	0.03	0.05	0.12
8.900	90.96	-35.55	0.04	0.03	0.05	0.12
8.950	91.26	-33.14	0.04	0.03	0.05	0.12
9.000	91.56	-31.29	0.04	0.03	0.05	0.12

Figures 8, 9, and 10 below show plots of the rotation angle, cross-polarized field magnitude, and insertion loss dependence on frequency:

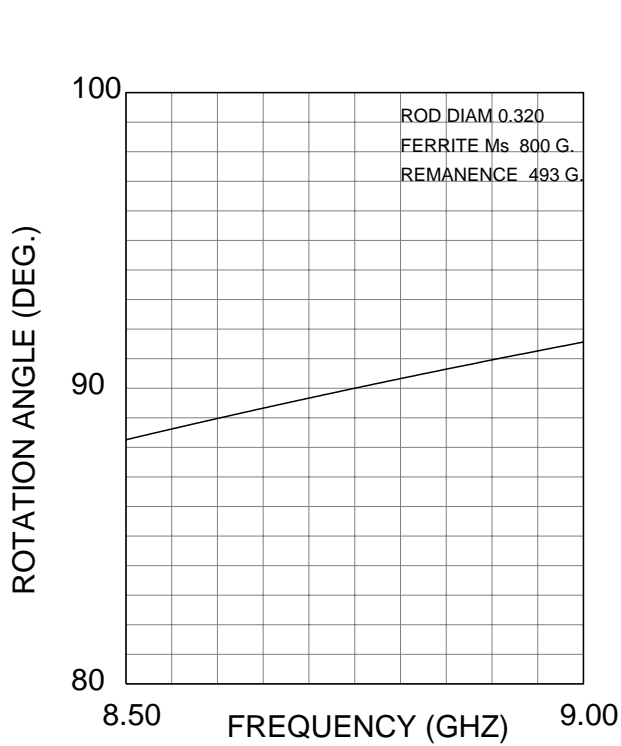


**Fig. 8 - Faraday Rotation Amount**

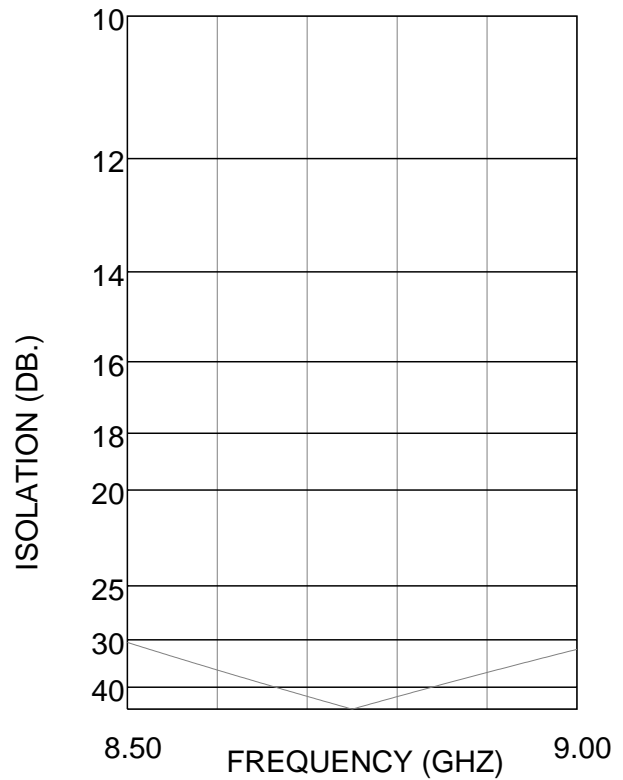


**Fig. 9 - Rotator Cross-Polarized Field**

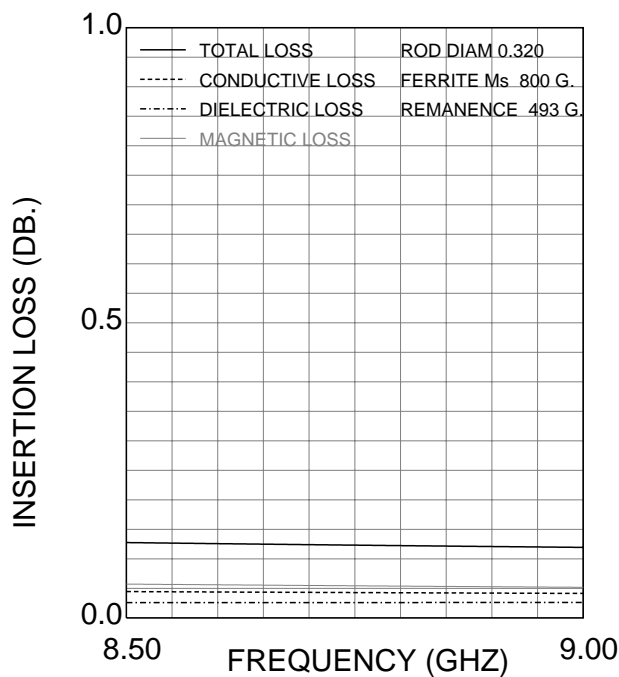


**Fig. 10 - Faraday Rotator Insertion Loss**

The frequency bandwidth of a practical Faraday Rotator is limited by impedance-matching problems and by the dispersion of the phase difference between the right-hand and left-hand circularly polarized normal modes. Impedance matching of the fully filled ferrite guide to a rectangular air-filled guide is usually done by using a section of ceramic dielectric rod that forms an extension of the ferrite rod. This ceramic rod projects through the end wall into the rectangular guide for some distance. The diameter, length, and dielectric constant of the projecting ceramic rod are adjusted empirically until a good impedance match is attained. This simple approach is adequate to match the phase shifter over a ten or twelve percent bandwidth to about 20 dB. return loss. The same technique is used to match the rotator output to square waveguide when the power levels are high enough to require incorporation of orthogonal mode transducers and external loads to absorb the cross-polarized error power. However, it is more difficult to achieve wide impedance match bandwidth because of the greater difference between characteristic impedance levels of the ferrite rod and the square guide.

The insertion loss of a rotator depends on the rod diameter, the dielectric and magnetic loss tangents of the material, the wall conductivity, and of course the deviation of the Faraday Rotation amount from the optimum level. The base dielectric loss is typically negligible compared with the magnetic loss and wall loss. In a well-designed low-power structure, the magnetic loss is usually largest, followed by the conductive loss, with the magnetic loss decreasing as the frequency is increased. When materials with a large spin-wave linewidth are used to raise the peak power threshold for onset of insertion loss increases, the magnetic loss at a given saturation moment also increases and may begin to dominate. For this reason, it is preferable to use a lower activity material and allow the length to increase somewhat so that the magnetic loss can be significantly reduced at the expense of a slight increase in wall loss. Stretching the ferrite rod length can also be beneficial by providing a greater surface area for extracting heat from the ferrite in high average power applications.

### 3. Switching Considerations

As with other design considerations, switching of Faraday Rotators follows closely the approach used with dual-mode phase shifters, with a few notable differences. While the dual-mode phase shifter usually operates at many different partially-switched states to provide many-bit phase control, the Faraday Rotators usually need to switch only between two values of rotation, e. g. +90 and -90 degrees. The maximum remanent magnetic flux value is used in the dual-mode phase shifter as a reference point for resetting the device prior to establishing a desired phase state by switching a predetermined amount of flux away from that reference. For the simplest Faraday Rotation switches, the  $\pm 90$  degree operating points are designed to be at the maximum limits of remanent flux.

The hysteresis loop shown in Figure 11 represents the B-H characteristic in the rotator rod with external return path elements. In this drawing, State 1 and State 2 are the major-loop maximum remanent operating points that provide equal magnitudes and opposite directions of bias magnetic flux. Note that the total magnetic flux is the flux density B integrated over the transverse-plane area of the rotator rod. For the simplest switch configuration, these states should ideally correspond to clockwise and counterclockwise rotations of 90 degrees in the rod. To switch between the two states, a voltage of the correct polarity is applied to the coil and the flux in the rod changes at a rate directly proportional to the instantaneous applied voltage and inversely proportional to the number of turns in the coil. The coil current is proportional to H integrated over the length of the closed magnetic path. Since  $H=0$  at State 1 and State 2, no steady current is needed in the quiescent case. Current will flow during the switching transient because H is nonzero. The magnitude of the current waveform versus time will generally have the shape shown in Figure 12, with the

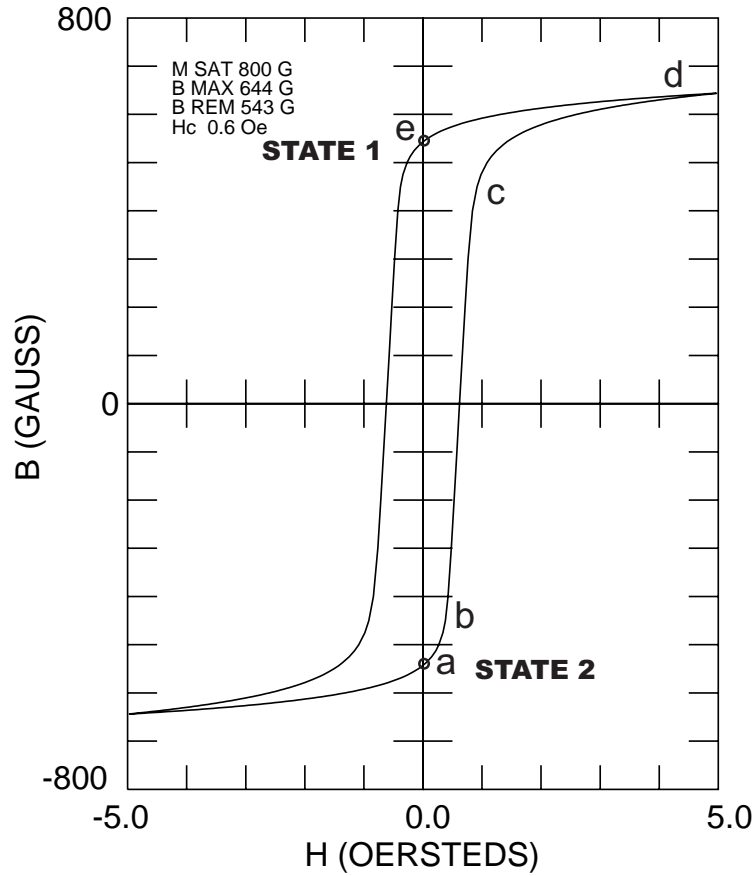


**Fig. 11 - Sample Hysteresis Loop**

points a through e matching the designations on the hysteresis loop of Figure 11. The voltage pulse ends at point d when the current reaches a preset level. Although one of the two rotator channels of the basic switch remains at the same state, its coil is pulsed with the same voltage polarity during each switching operation. Because the flux density level of the ferrite for this channel is already at the knee of the hysteresis loop, the current will rise rapidly to the preset value for terminating the voltage pulse. Sensing of the current rise to the preset limit in both channels is typically used as an indication that the ferrite is being switched normally, and a built-in-test error signal is generated when the desired current limit is not sensed in a channel.

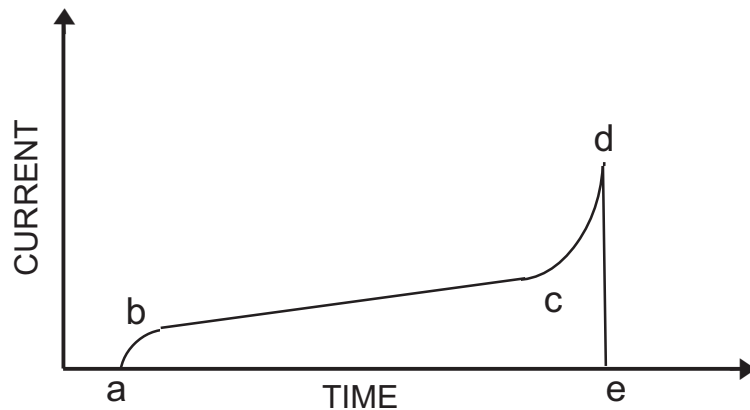


**Fig. 12 - Switching Current Waveform**

Figure 8 above showed that the amount of Faraday Rotation for a practical ferrite will vary as a function of frequency. It is well known that the magnetic properties of ferrite materials also change with temperature. The combination of these factors will limit the frequency and temperature range over which the rotation error angle will be small enough to meet a given criterion of added insertion loss when major-loop switching is used. Figure 13 shows a scaled plot of measured major-loop latching Faraday Rotation angle range data for a standard temperature-compensated garnet material. The optimum value for the  $\pm 90$  degree rotator is of course 180 degrees. If an added insertion loss of 0.15 dB. maximum is allowed, then the temperature of the rotator must be constrained to the range zero to fifty-seven degrees Celsius to keep from exceeding that value at all temperatures and frequencies. It is clear that operation over wider temperature-frequency ranges cannot be attained without serious degradation of insertion loss using major-loop switching.

The way around this problem is once again to borrow from existing knowledge about control of dual-mode latching phase shifters by introducing metered-flux switching. In this scenario, one end of the hysteresis loop is used as a reference, and flux is switched away from that reference to a point near the opposite end of the loop which will provide the latching flux level needed to achieve the desired Faraday Rotation angle. That is, the flux change is controlled by a timed voltage pulse applied to the coil rather than by sensing a predetermined saturation current level. A temperature sensor is used to adjust the pulse length to compen-

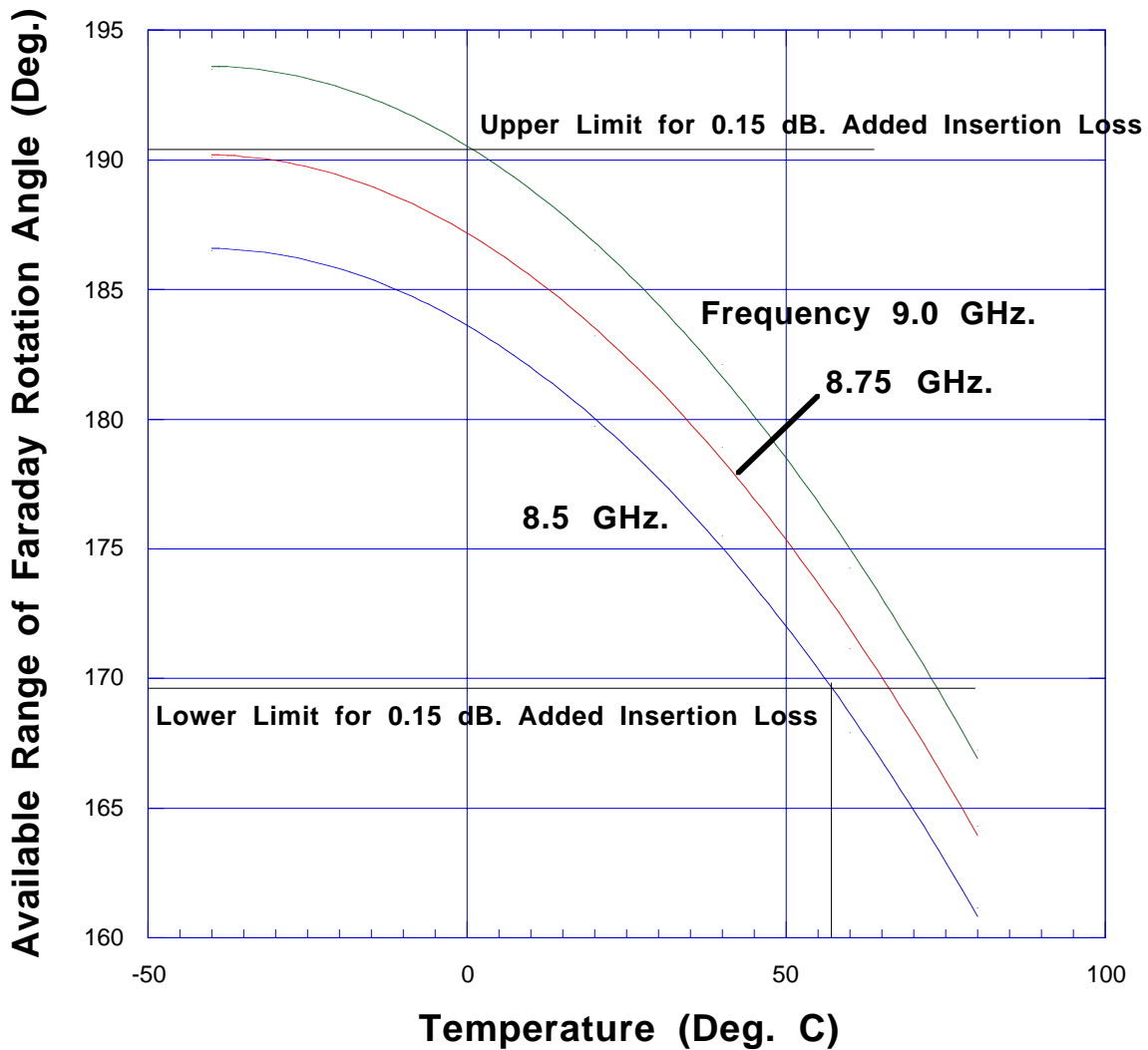
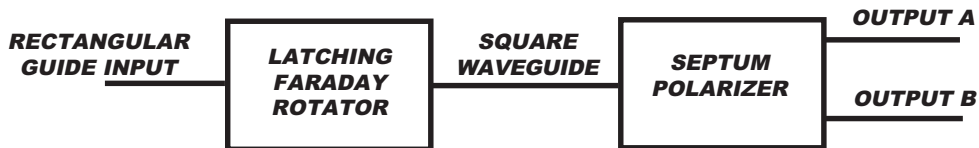


Fig. 13 - Available Latching Rotation Angle vs. Temperature and Frequency

sate for stretching or shrinking of the material hysteresis loop caused by temperature changes. Now the design criterion for the ferrite material length becomes one of assuring that the available latching Faraday Rotation angle does not fall below the optimum 180 degrees at the highest operating temperature of the switch. The rotator that does not change state must always be switched from the reference to the state near the opposite end of the hysteresis loop, while the rotator that does change state alternates ends for reference and operating points. Note also that during changes of temperature, the operating point of the rotators will drift from optimum values, and it is necessary to set the rotators again to restore full performance at the new temperature.

The discussion above used data measured on the available rotation angle of Faraday Rotators. Direct measurement of the angle in space is a tedious process not compatible with ordinary laboratory practice and measurement equipment. The block diagram of Figure 14 shows a very convenient way of handling the problem. An input signal is coupled to the rotator and receives a particular amount of angle rotation. The output of the rotator is coupled to square waveguide, and then into the square guide end of a septum polarizer. An ideal septum polarizer separates linearly polarized waves input to the square guide into equal-amplitude waves at its two rectangular waveguide ports, identified as Output A and Output B in Figure 14. Furthermore, the phases of the waves in the two outputs are in one-to-one correspondence with the rotation angle of the wave entering the square guide. When the input polarization angle is changed by an amount  $\theta$  the phases in the two rectangular guides will change by  $+\theta$  and  $-\theta$ , respectively. Measurement of the rotation angle is replaced by measurement of a correlated phase angle, a much easier task that can be accomplished readily using a standard Network Analyzer. By varying the control current of the rotator from negative to positive magnetic saturation and back, curves of the type shown in Figure 15 can be generated.



**Fig. 14 - Measurement of Latching Rotation Angle**

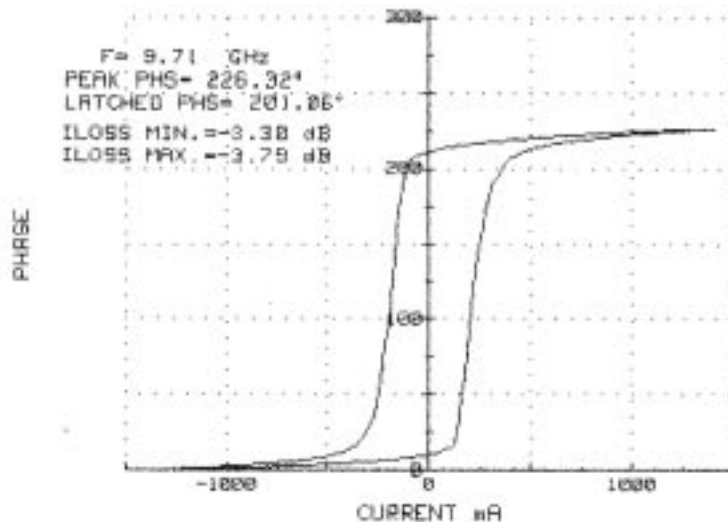


**Fig. 15 - Hysteresis Loop of Rotation Angle**

#### 4. High Power Considerations

There are two distinct high power concerns in ferrite devices, those associated with peak power effects and those associated with heating from high average power. First and foremost is the need to select a material that will not be driven by peak r-f power beyond the threshold for onset of high insertion loss caused by electron spin instability. As discussed above, the usual approaches for increasing the threshold power level are (a) to broaden the spinwave linewidth of the material by using a material with high gadolinium content or doped with a small amount of holmium or dysprosium, and/or (b) to use a material with a lower saturation magnetization. Increasing the material spinwave linewidth usually causes the low-power insertion loss to increase somewhat, while reducing the material saturation moment requires a longer interaction region, leading to a bigger and heavier device, and also may cause the temperature dependence to increase.

Another peak-power effect that needs to be considered is high-voltage breakdown, i. e. arcing. In order to permit fast switching with minimal shorted-turn effects, the ferrite elements are usually coated with a thin sputtered metallization which forms a fully-filled circular waveguide. Any minute weaknesses or breaks in this sputtered metallization can lead to r-f arcing at high peak power. Therefore the integrity of this coating must be high and must be preserved throughout the assembly steps that follow the initial sputtering. Careful cleaning and in some cases impregnation of porous materials prior to sputtering is helpful, and avoidance of contamination or abrasion during the subsequent handling is essential.

In extreme cases, high average power levels can lead to fracture of the ferrite material because of stresses resulting from large internal temperature gradients. For a sufficiently long rod of circular cross-section with uniform heat generation, the spatial variation of temperature T can be taken as one-dimensional, i. e. in the radial direction only, and the steady-state distribution will be [4]

$$T(r) = \frac{g}{4K} \left[ \frac{d^2}{4} - r^2 \right] \quad (r \leq d/2) \quad (5)$$

where T = Temperature rise above the exterior surface temperature, °F  
g = Heat generation density, W/in.<sup>3</sup>  
K = Rod material thermal conductivity, W/(in. °F)  
d = rod diameter, in.  
r = radial distance from rod axis, in.

This expression is a parabola with maximum gradient at  $r = d/2$  of

$$\left. \frac{dT}{dr} \right|_{r=d/2} = \frac{gd}{4K} \quad (6)$$

Practical high power ferrite rod devices have operated at gd values of at least 100 watts/in.<sup>2</sup> without fracture, which implies fracture-free average power handling capability in excess of 10 kW for well-designed rotators at C-band and above.

Consequently the main concern for cases of high average power will be to provide some means of extracting heat from the ferrite rod so that the temperature rise can be held to a reasonably low value. Figure 16

shows a rotator rod cross-section with heat sinks contacting the ferrite to provide a path for thermal conduction of heat dissipation from the rod to the external case of the device.

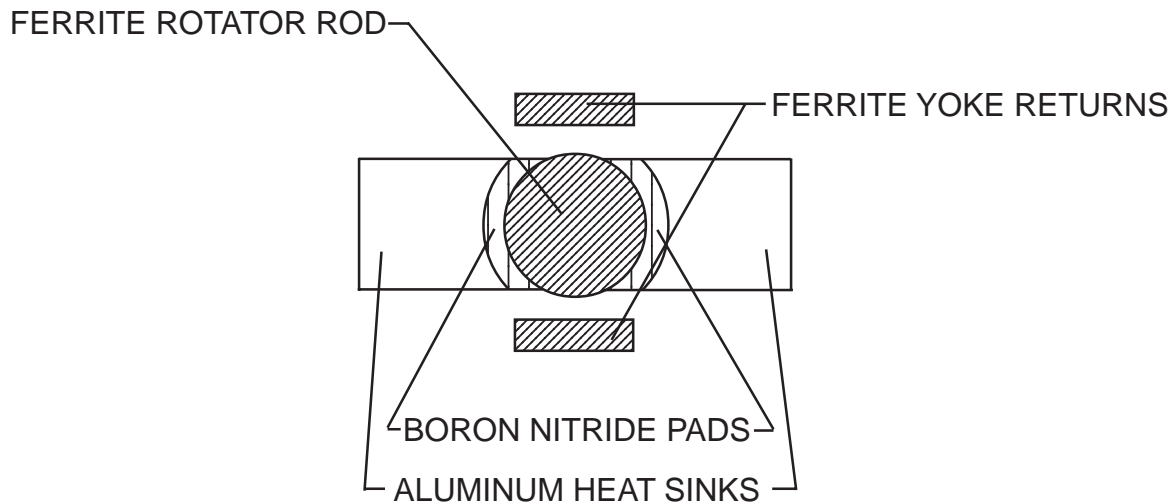


**Fig. 16 - Latching Rotator Rod Heat Sink Cross-Section**

As a final note regarding high power handling, it should not be forgotten that the bridge-type configuration being presented here requires each rotator to handle only half the input power.

### 5. SP3T Switch Variant

Review for a moment the block diagram of Figure 6, which uses orthogonal mode transducers to couple off any cross-polarized error power. If a third state, namely zero rotation, is added to the rotators, all the power will be coupled to the cross-polarized arms of the orthomode transducers. These outputs can be summed in another hybrid tee, thereby providing three usable outputs from the rotator bridge configuration. Figure 17 shows a block diagram of the revised arrangement.

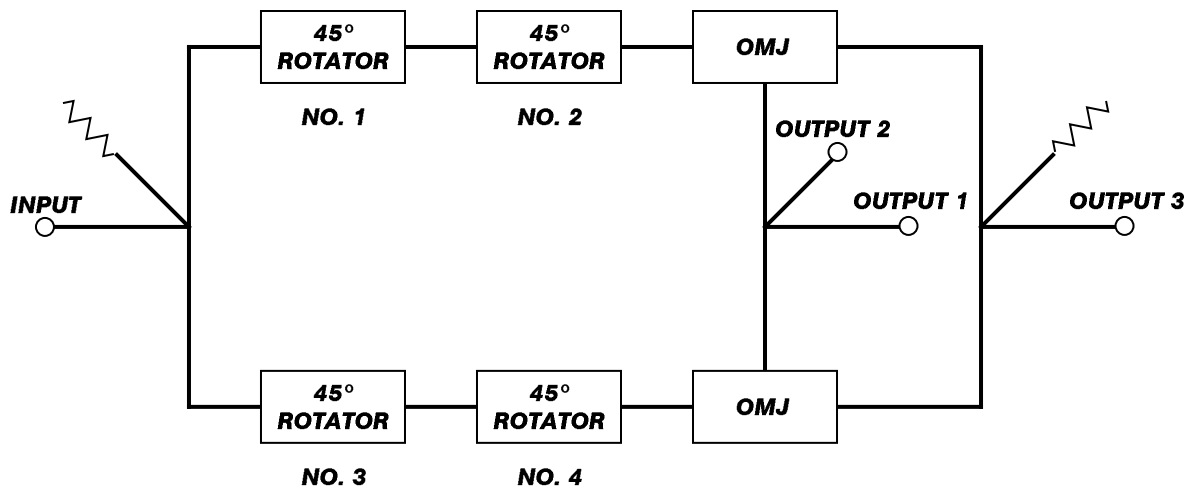
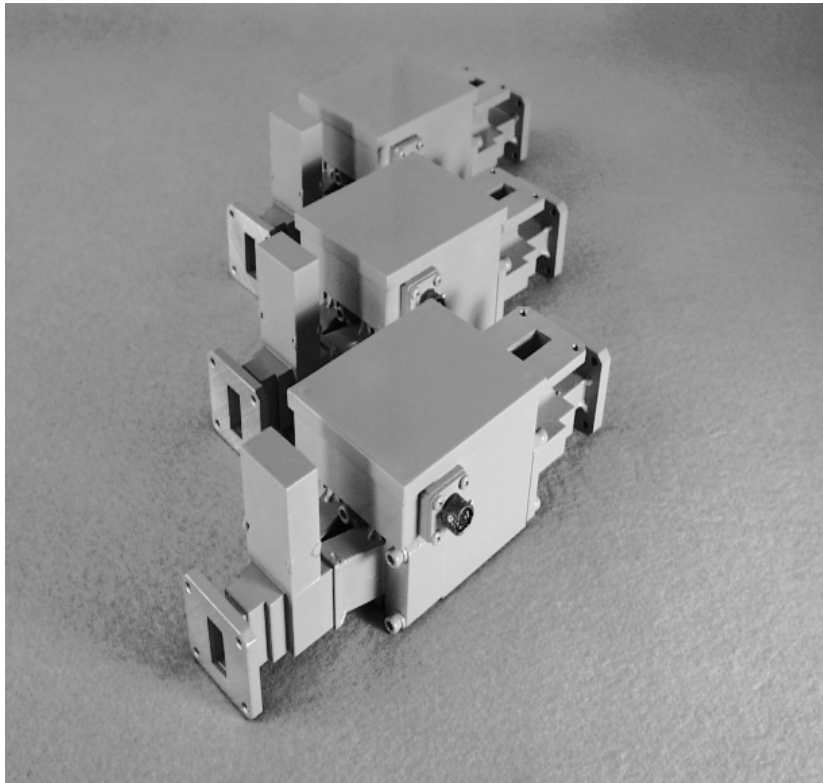


**Fig. 17 - SP3T Switch Variant Block Diagram**

A practical realization of the three-state rotator is achieved by connecting two identical  $\pm 45$  degree rotators in tandem. The zero-rotation state is attained by driving each tandem pair into major-loop remanence, but in opposite directions. This state also establishes a “reset” reference from which metered-flux switching can be carried out to set the 90 degree rotation states accurately. Note that any cross-polarized error for the 90 degree states may be coupled directly to the zero rotation port, and so the isolation curve of Figure 2 applies for this case. Therefore greater care must be taken to ensure that the 90 degree rotation angle values are set with sufficient accuracy.

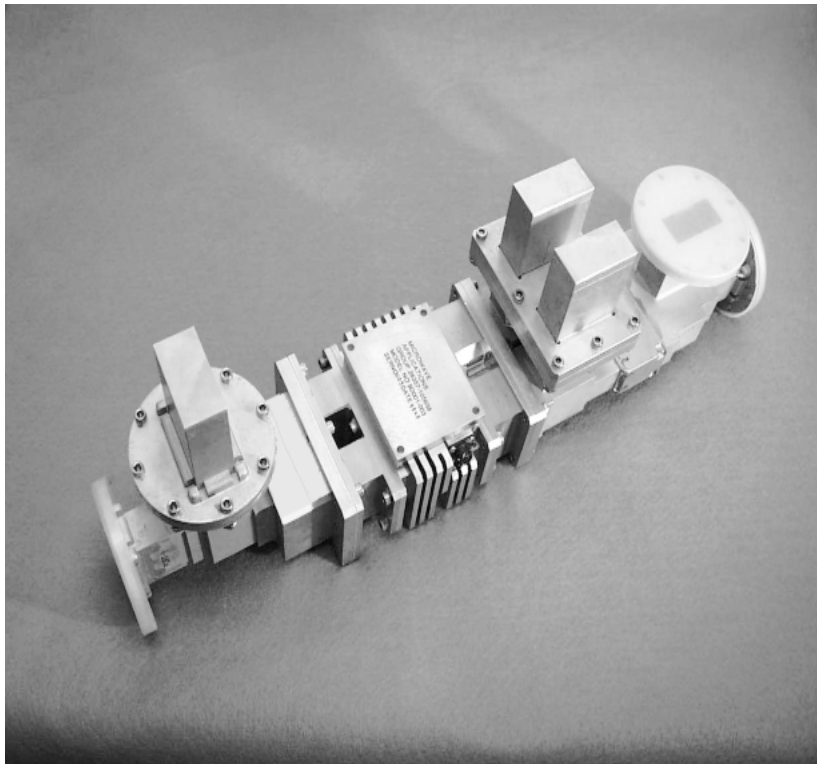
## 6. Practical Hardware

Figures 18 through 20 show practical hardware implementations of the design principles outlined above.



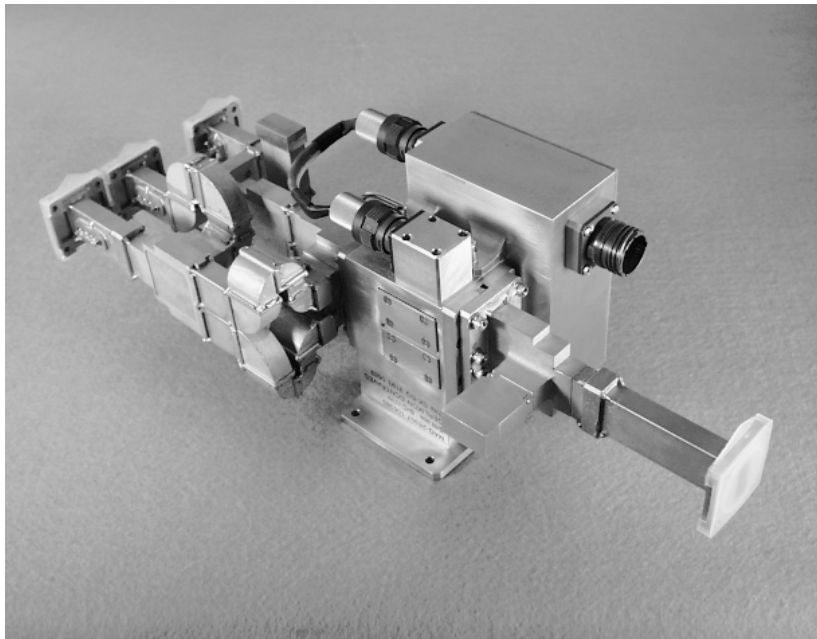
**Fig. 18 - Simple X-Band Switch**

Figure 18 above shows an X-band switch using the basic block diagram of Figure 3 with internal film loads to absorb cross-polarized error angle energy, and with major-loop switching. This switch is rated to operate with 50 kW peak power, 50 W average power, with an insertion loss of 0.5 dB. maximum. Because the operating bandwidth is narrow (2% bandwidth) an operating temperature range from  $-29\text{ }^{\circ}\text{C}$  to  $+49\text{ }^{\circ}\text{C}$  is available. Return loss is specified at 17 dB. maximum, and isolation at 25 dB. minimum, although typical values are higher. Switching time of 50 microseconds and switching rate of 4,000 operations per second are achieved with this unit.



**Fig. 19 - C-Band Switch with External Loads**

Figure 19 above shows a C-band switch using the robust block diagram of Figure 6 with orthogonal mode transducers and external loads to absorb cross-polarized error angle energy, and also with major-loop switching. This switch is rated to operate with 300 kW peak power, 300 W average power, with an insertion loss of 0.6 dB. maximum. A 4% operating bandwidth is offered over an operating temperature range from -40 °C to +50 °C. Return loss is specified at 20 dB. maximum, and isolation at 30 dB. minimum, although typical values are higher. Switching time of 50 microseconds maximum and switching rate of 1,500 operations per second are achieved with this unit.



**Fig. 20 - X-Band SP3T Switch Variant**

Finally, Figure 20 shows an X-band SP3T variant switch using the block diagram of Figure 17 with orthogonal mode transducers, three-state rotators, and metered-flux switching. This switch is rated to operate with 25 kW peak power, 250 W average power, with an insertion loss of 1.0 dB. maximum. A 10% operating bandwidth is offered over an operating temperature range from -40 °C to +71 °C. Return loss is specified at 15 dB. maximum, and isolation at 20 dB. minimum, although typical values are higher. Switching time of 50 microseconds maximum and switching rate of 1,200 operations per second are achieved with this unit.

## 7. Conclusions

Switching junction circulators have been assigned many tasks for controlling the direction of microwave power flow. However, there are some applications where Faraday Rotators in a bridge circuit can provide distinct advantages. For example, it is awkward to build reciprocal switches using junction circulators, but easy with the rotator bridge. Power dissipation is highly concentrated in junction circulators, which are essentially low-Q resonators, but can be distributed in the rotators, which are transmission line devices. This allows heating to be carried away more readily by the heat-sinking approach described above. The non-planar mode available for the rotator bridge allows a simple three-way switch to be constructed using only two ferrite elements. By selecting matched pairs of ferrite rotators, balance of the bridge can be maintained over a wide range of temperatures, frequencies, and power levels. And last but not least, power is divided in the bridge so that each rotator element needs to handle only half the input power to the switch.

## 8. References

- [1] E.A. Ohm. "A Broad-Band Microwave Circulator." 1956 Transactions on Microwave Theory and Techniques, vol 4, no. 4 (Oct. 1956 [T-MTT]); pp. 210-217.
- [2] C.R. Boyd, Jr.. "A Dual-Mode Latching Reciprocal Ferrite Phase Shifter." 1970 Transactions on Microwave Theory and Techniques, vol.18, no.12 (Dec. 1970 [T-MTT] (1970 Symposium Issue)); pp. 1119-1124.
- [3] C.R. Boyd, Jr.. "Comments on the Design and Manufacture of Dual-Mode Reciprocal Latching Ferrite Phase Shifters." 1974 Transactions on Microwave Theory and Techniques, vol. 22, no. 6 (Jun. 1974 [T-MTT] (Special Issue on Microwave Control Devices for Array Antenna Systems)); pp. 593-601.
- [4] C.R. Boyd, Jr., L.R. Whicker and R.W. Jansen. "Study of Insertion-Phase Variation in a Class of Ferrite Phasers." 1970 Transactions on Microwave Theory and Techniques, vol. 18, no.12 (Dec. 1970 [T-MTT] (1970 Symposium Issue)); pp. 1084-1089.